engineering proceedings

MDPI

Proceeding Paper

Experimental Evaluation of Thermal Performance in Shell and Tube Heat Exchangers Using Al_2O_3-γ Nanofluids †

Shahid Iqbal [1], Muhammad Faisal Naveed [1,*], Manzar Masud [2], Adnan Tariq [1], Taimoor Kausar [1], Zohaib Nasir [1] and Moazzam Ali Babar [1]

[1] Mechanical Engineering Department, Wah Engineering College, University of Wah, Wah Cantt 47040, Pakistan; shahid.iqbal@wecuw.edu.pk (S.I.); adnan.tariq@wecuw.edu.pk (A.T.); taimoorawan611@gmail.com (T.K.); zohaibnasir324@gmail.com (Z.N.); moazzamali0105@gmail.com (M.A.B.)
[2] Department of Mechanical Engineering, Capital University of Science and Technology, Islamabad 44000, Pakistan; manzar.masud@cust.edu.pk
* Correspondence: muhammadfaisalnaveed6@gmail.com
† Presented at the 4th International Conference on Advances in Mechanical Engineering (ICAME-24), Islamabad, Pakistan, 8 August 2024.

Abstract: Shell and tube heat exchangers (H.Xs) are being used broadly in the generation of power, refrigeration, nuclear, chemical, and petroleum industries due to their high cooling and heating capacity. In this research paper, an experimental test bench for a shell and tube H.X was fabricated according to the standard. This study aimed to test the thermal performance of shell and tube H.Xs using Al_2O_3-γ nanofluid with different concentrations in counter flow configurations. Nanoparticles of 12 nm of size and 99% purity were used in this investigation. These nanoparticles were dispersed in distilled water to prepare nanofluids at three different concentrations: 0.11%, 0.22%, and 0.34%. Nanofluids of different concentrations were heated and passed through H.X tubes while water was passed through the shell side. The experiments were performed at three different flow rates: 6, 8, and 10 L per minute (L/min). It was observed from the experimentation that nanofluid has higher efficiency as compared to simple distilled water. Experimental investigations showed higher values of overall heat transfer coefficient (U), convective heat transfer coefficient (h), and heat transfer rate ($\dot{Q}$) at 0.22%, noted as 33.33%, 48%, and 30%, respectively. The lowest value for U was noted 47% for distilled water. The hydrodynamic and thermal boundary layers were also determined, and when the flow rate increased it led to thinning of the thermal boundary layer and improved heat transfer; however, increased concentrations of nanoparticles thickened the boundary layer by increasing viscosity and boosting thermal conductivity (k) simultaneously. It was revealed that the best concentration for maximizing heat transfer was 0.22%. The findings show that heat transmission efficiency was improved at both 0.11% and 0.22% of nanofluids compared to simple distilled water; when the concentration was raised to 0.34%, the results decreased due to increasing viscosity. Therefore, there is a need to precisely adjust the nanoparticle loading rate for maximum heat transfer enhancement without affecting fluid properties.

Keywords: heat exchangers; nanofluid; heat transfer; thermal conductivity; overall heat transfer coefficient; LMTD

check for updates

Citation: Iqbal, S.; Naveed, M.F.; Masud, M.; Tariq, A.; Kausar, T.; Nasir, Z.; Babar, M.A. Experimental Evaluation of Thermal Performance in Shell and Tube Heat Exchangers Using Al_2O_3-γ Nanofluids. *Eng. Proc.* **2024**, *75*, 13. https://doi.org/10.3390/engproc2024075013

Academic Editors: Muhammad Mahabat Khan, Muhammad Irfan and Mohammad Javed Hyder

Published: 24 September 2024

Copyright: © 2024 by the authors. Licensee MDPI, Basel, Switzerland. This article is an open access article distributed under the terms and conditions of the Creative Commons Attribution (CC BY) license (https://creativecommons.org/licenses/by/4.0/).

1. Introduction

Heat exchangers facilitate the efficient transfer of heat from one medium to another. Shell and tube H.Xs are being used broadly in most industrial applications, including energy conversion, evaporators, condensers, heating, cooling, ventilation, and power utility systems. A number of goals have been pursued by researchers, including increasing fuel and energy efficiency, decreasing heat transmission times, lowering the size, weight, and cost of heat exchangers, and eliminating energy losses. A heat exchanger's performance may be increased by a number of techniques, including the use of microchannels and fins.

The ability to transport heat can also be improved by making the working fluid more thermally conductive [1]. When comparisons are made to the thermal conductivity (k) of solids, the fluids that used to be used for the transmission of heat such as water, motor oil, vegetable oil, paraffin oil, propylene glycol, ethylene glycol, etc., have poor thermal conductivities [2]. A base fluid's k can be raised through the mixing of some highly thermally conductive solid particles. Recently, modifying the heat transmission characteristics of suspensions by the use of nano-sized particles has drawn interest. Nanofluids are stable suspensions of particles in traditional heat transmission fluids that are less than 100 nm in size. When compared to other suspensions, nanofluids exhibit superior stability, a very high k level, and no additional pressure loss, making them a viable option for engineering applications. Research has been conducted on the k of nanofluids, as it is one of the most crucial factors for improving heat transmission. Every experiment's outcome has shown that the inclusion of nanoparticles increases heat conductivity [3].

Li and Xuan conducted multiple experimental studies on the heat transmission and flow properties of cupric oxide nanofluids. The trials were conducted in a linear conduit with a consistent thermal boundary condition. Several researchers conducted their studies under two separate flow regimes, namely laminar and turbulent flow conditions [4,5]. A comprehensive investigation by R. Subramanian et al. revealed that a heat transmission increase of 5–25% was obtained using the nanofluids of TiO_2 nanoparticles, respectively. The results of the study demonstrated a significant connection between heat transmission enhancement, mass flow rate, and nanofluid volume concentration. Because the surface area was increased by the nanoparticles, the heat transfer rates improved [6]. Farajollahi et al. performed an experimental assessment of heat transmission in a shell and tube H.X by dispersing CO_2 nanoparticles and Al_2O_3 nanoparticles in water. The examination revealed that the h of the nanofluids containing Al_2O_3-water and TiO_2-water rose by 19 to 56% and 18 to 56%, respectively, at 0.3 to 2% concentrations [7,8]. The impact of the concentration and proportion of nanoparticles on heat transmission performance was examined in S. Anitha's research employing a shell and tube H.X and Al_2O_3-Cu hybrid nanofluids dispersed in water. The results concluded that the h and the Nusselt number (Nu) increased steadily as the concentration was raised; there was a noteworthy 139% increase in h when compared to water and a 25% increase when compared to Cu/water nanofluids [9].

An extensive literature [4–9] exists regarding heart transfer assessments for various heat exchangers using different working fluids with various concentrations of nanoparticles. There is no research article available for finding U, Reynolds number (Re), h, and k using the LMTD method for a shell and tube H.X using water-based Al_2O_3-γ nanofluids with concentrations of 0.11%, 0.22%, and 0.34% for counter flow. Therefore, the purpose of this study is to determine the thermal performance of a shell and tube H.X using an Al_2O_3-γ nanofluid with different concentrations in counter flow configuration. Nano-particles of 12 nm of size and 99% purity are used in this study.

By examining the performance of nanofluids in a shell and tube H.X under novel operating circumstances and of low-concentration Al_2O_3-γ nanoparticles distributed in water, this work aims to close the knowledge gap identified in earlier studies.

2. Experimental Procedure

2.1. Experimental Apparatus

The setup that was used for experimentation consisted of a shell and tube H.X containing 19 tubes, with a length of 300 mm, made of copper material, and arranged in triangular pattern. The shell and tube H.X contained 6 baffle plates spaced with 43 mm distance from each other; the types of baffles were single segmental with a 30% cut, the internal diameter of the tubes was 12 mm, and the diameter of the shell was 90 mm. The setup contained two flow meters (rotameters) of an 18 L/min capacity, one for flow in tubes and one for flow in shell. Four K-type thermocouples were installed in both inlets and outlets of the shell and tubes. The setups contained two 0.5 hp pumps, two water reservoirs with a 30 L capacity, and one 1.5 KW heater.

For the experimentation process, the hot fluid (nanofluid) was passed through the tubes, and cold fluid was passed through the shell and tube H.X; the range of the flow rate was 6, 8, and 10 L per minute which was measured with the help of rotameters. The heat exchanger was configured in a counter flow arrangement. The specifications of various components of the shell and tube H.X test apparatus are given in Table 1. The diagram of shell and tube H.X apparatus and tube arraignments with baffles are shown in Figure 1a,b.

Table 1. Specifications of the shell and tube H.X apparatus.

Components	Specifications
Inside Dia of shell	90 mm
Thickness of shell	5 mm
Shell material	Steel
Length of tubes	300 mm
Tubes material	Copper
Tubes inside Dia	12 mm
Tubes thickness	1 mm
No of baffles	06
Baffles spacing	42.8 mm
Baffles cut	30%
Baffle type	Single segmental
Tubes arrangement	Parallel triangular with 30° Angle

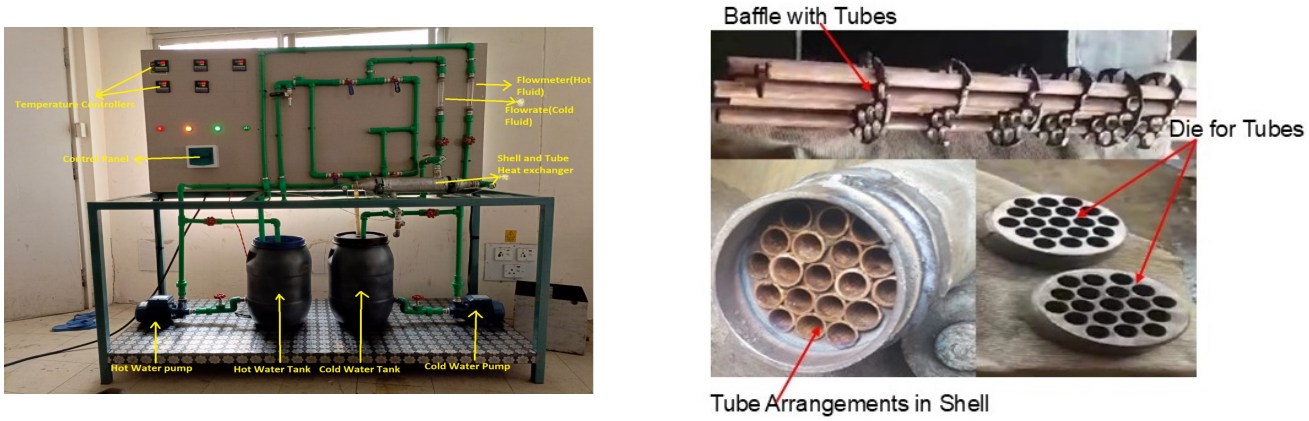

(**a**) (**b**)

Figure 1. (**a**) A diagram of the shell and tube H.X apparatus; (**b**) the tube arrangement in the shell with baffles.

2.2. Preparation of Al_2O_3-γ Nanofluid

Al_2O_3-γ nanoparticles with a diameter of 10–15 nm were used for the preparation of the nanofluid. The nanoparticles were purchased from the Jiangsu XFNANO Materials Tech Co., Ltd. (Nanjing, China). The base fluid utilized in this process was distilled water. Utilizing a magnetic stirrer, the nanoparticles were constantly stirred for 90 min to evenly distribute them throughout the base fluid, and then these nanoparticles were sonicated using a stalwart sonicator. An exact volume concentration of 14 L of nanofluid was prepared for this investigation, and the particle weight was measured using a TS2000 weight scale, (Jiangyin Suofei Electronic Technology Co., Ltd., Jiangyin, China). In this work, Al_2O_3-γ nanoparticles at volume concentrations of 0.11, 0.22%, and 0.34% were used. An SEM image of the Al_2O_3-γ nanoparticles and the magnetic stirrer used for dispersion of nanoparticles are presented in Figure 2a–c. The thermophysical properties of nanoparticles are given in Table 2.

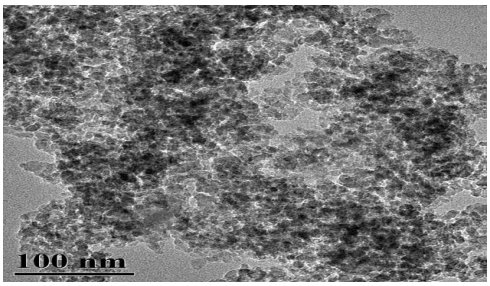

(**a**)

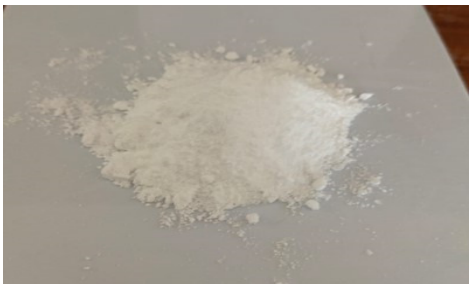

(**b**)

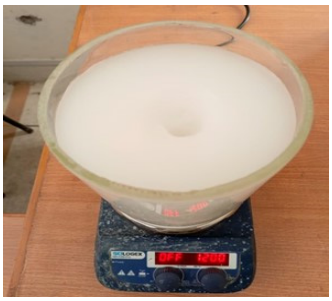

(**c**)

Figure 2. (**a**) SEM image of Al_2O_3-γ nanoparticles; (**b**) Al_2O_3-γ nanoparticles; (**c**) dispersion process of nanoparticles using magnetic stirrer.

Table 2. Thermophysical properties of the nanoparticles.

Nanoparticles	Diameter (nm)	Specific Surface Area (m^2/g)	Density (kg/m^3)	Specific Heat Capacity) (J/kg·K)	Thermal Conductivity (W/m·K)
Al_2O_3-γ	12	120	3690	880	18

The thermal conductivity of nanofluids was calculated using the Maxwell model [10].

$$\frac{K_{nfd}}{K_{water}} = \frac{K_{npr} + 2K_{water} + 2\varnothing(K_{npr} - K_{water})}{K_{npr} + 2K_{water} - \varnothing(K_{npr} - K_{water})} \quad (1)$$

where K_{nfd} is the conductivity of the nanofluid, K_{npr} is the conductivity of the nanoparticle, and ∅ is the concentration of the nanoparticles dispersed in water.

The viscosity of the nanofluid was calculated using the Einstein equation [11] which is as follows:

$$\mu_{nfd} = [1 + 2.5(\varnothing)]\mu_{water} \quad (2)$$

where μ_{nfd} is the viscosity of the nanofluid.

To find the density of the nanofluid, the equation introduced by Pak and Cho [12] was used:

$$\rho_{nfd} = (1 - \varnothing)\rho_{water} + (\varnothing)\rho_{npr} \quad (3)$$

where ρ_{nfd} and ρ_{npr} are the densities of the nanofluid and nanoparticles, respectively.

The heat capacity (C_p) of the nanofluid is given by [4] the following equation:

$$C_{p,nfd} = \frac{(\varnothing)(\rho C_p)_{npr} + (1 - \varnothing)(\rho C_p)_{water}}{\rho_{nfd}} \quad (4)$$

where $(\rho C_p)_{npr}$ and $(\rho C_p)_{water}$ are the nanoparticles and the base fluid, water.

2.3. Heat Transfer Coefficient

The heat transmission rate, U, and the convective h of the nanofluid were determined using 6, 8, and 10 L/min of nanofluid with concentrations of 0.11%, 0.22%, and 0.34%, and water. The rate of heat transmission of a hot fluid is expressed as follows:

$$\dot{Q} = \dot{m} c_p (T_{hi} - T_{ho}) \tag{5}$$

where $\dot{m}$ is the mass flow rate, c_p is the specific heat capacity, T_{hi} is the hot water inlet, and T_{ho} is the hot water outlet; U is expressed as follows:

$$\mathrm{U} = \frac{\dot{Q}}{\mathrm{A} \times \Delta \mathrm{T}_{LMTD}} \tag{6}$$

where A is the area of heat transmission and $\Delta \mathrm{T}_{LMTD}$ represents the logarithmic mean temperature difference. Furthermore, the Nusselt, Reynolds [13], and Prandtl numbers [3] of the fluid on the tube side were approximated as follows:

$$\mathrm{Nu}_{nfd} = \frac{\mathrm{hD}}{K_{nfd}} \tag{7}$$

$$\mathrm{Re}_{nfd} = \frac{\rho_{nfd} \mathrm{V}_{nfd} \mathrm{D}}{\mu_{nfd}} \tag{8}$$

where V_{nfd} represents the velocity of the nanofluid and D is the diameter of the tube.

$$\mathrm{Pr}_{nfd} = \frac{\mu_{nfd} \mathrm{Cp}_{nfd}}{K_{nfd}} \tag{9}$$

The Hausen equation was also used [14].

$$\mathrm{Nu} = 3.66 \frac{0.0668 \left(\frac{\mathrm{D}}{\mathrm{L}}\right) \mathrm{Re}_{nfd} \times \mathrm{Pr}_{nfd}}{1 + 0.04 \left[\left(\frac{\mathrm{D}}{\mathrm{L}}\right) \mathrm{Re}_{nfd} \times \mathrm{Pr}_{nfd}^{\frac{2}{3}} \right]} \tag{10}$$

3. Results and Discussion

The thermal behavior of water and water-based nanofluids at various concentrations and flow rates was investigated. The findings showed that a higher k of the alumina oxide nanoparticles led to increases in the K of 26%, 44%, and 58% at nanoparticle concentrations of 0.11%, 0.22%, and 0.34%, respectively. The higher density of the nanoparticles added mass without significantly changing volume, and this increased the viscosity by 16%, 33%, and 44% at the same concentrations. The increased K of nanofluids requires less heat energy for a given temperature, and this resulted in a decrement of heat capacity of 24%, 67%, and 107%. The relation of U and concentrations is shown in Figure 3.

The U showed that different nanoparticle concentrations significantly improved heat transmission efficiency. Due to enhanced k and fluid dynamics, at a 0.11% nanofluid concentration, U increased by almost 16% when compared to water. U increased by over 33.33% at a concentration of 0.22%, indicating the ideal trade-off between fluid characteristics and nanoparticle dispersion to maximize heat transmission. Nevertheless, U only increased by 10% at a concentration of 0.34%, indicating diminishing returns brought on by rising fluid viscosity. The relation between convective h and concentrations is shown in Figure 4.

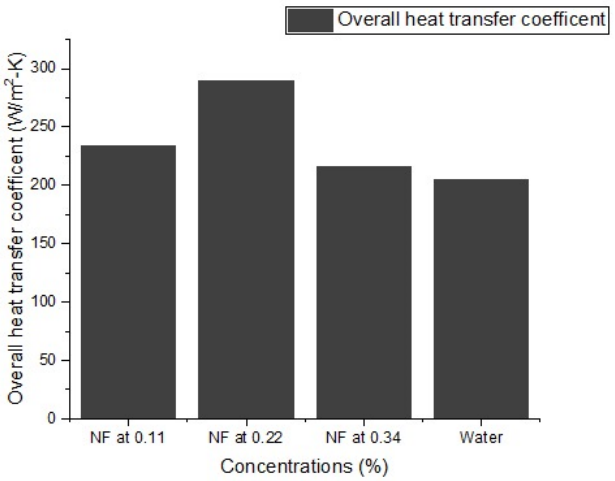

Figure 3. Relationship between mean U and concentrations of nanofluids.

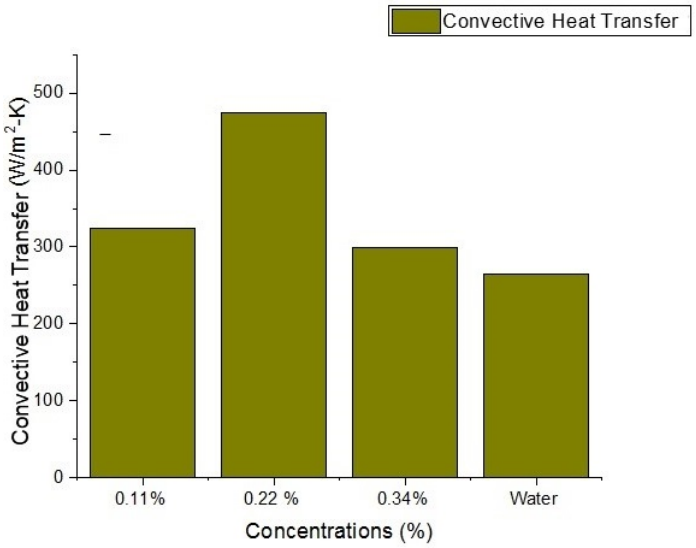

Figure 4. Relationship between mean h and concentrations of nanofluid.

Nanoparticle loading increased the heat exchanger convective heat transfer by 24.6% and 48% at 0.11% and 0.22% concentrations. The improvement was only approximately 14%, though, at 0.34% due to the increased viscosity, which adversely affects both heat transfer efficiency and fluid dynamics.

There were similar trends in the heat transfer rate as heat transmission increased by around 16% and 30%, respectively, at the 0.11% and 0.22% nanofluid concentrations as compared to water. At a 0.22% concentration, the nanoparticles were most uniformly dispersed throughout the base fluid, providing the highest surface area for heat transmission. The nanofluid's stability was probably at its peak around 0.22%, which maintains the fluid's consistent thermal characteristics and inhibits particle settling. Improved k results from this optimum dispersion also improved the interaction between the fluid and the nanoparticles. For experimental (U) and theoretical (h) values, the deviation of the volumetric concentration of 0.22% and water was noted as 38.81% and 22%, respectively. Alumina oxide nanoparticle addition resulted in improved heat transfer performance, as seen by the rising trends in both U and h with the nanofluid concentration. The relationship between the U and the flow rate at various concentrations and water is seen in Figure 5.

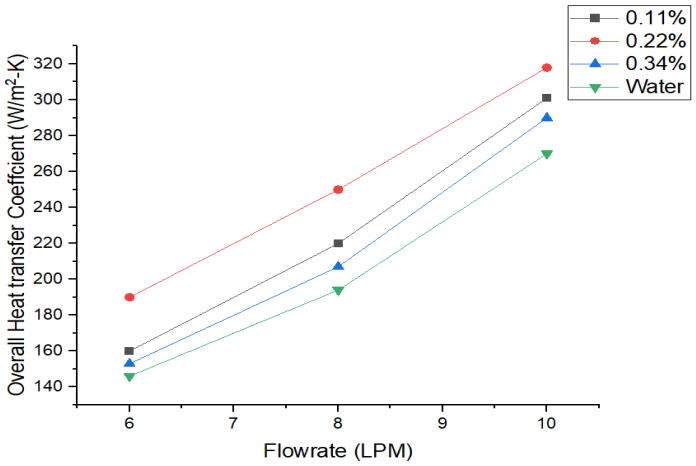

Figure 5. Relationship between U and different flow rates of water and nanofluids.

Figure 5 illustrates the effect of the alumina oxide nanoparticles' volume percentage and the flow rate on the total h. It shows a notable improvement in the h between a 6 and 10 L/min flow rate; for 6 L/min, there was a 14.2% increase at 0.11%, a 33.57% increase at 0.22%, and at 0.34% the increase was only 5.7%. Similarly, at 8 L/min and 0.11% the increase was 19%, at 0.22 the increase was 36%, at a 10 L/min flow rate the increase was 14.2% at 0.11,% and at 0.22% it was 23.8%. When compared to water, the Al_2O_3–H_2O nanofluid demonstrated about a 33% increase in U at the best concentration of 0.22%. The improved performance is attributed to the nanofluid's higher thermophysical properties compared to water, and also the high conductivity and stability of the fluid. The relation between the LMTD and the Reynold number at various volumes and water is shown in Figure 6a.

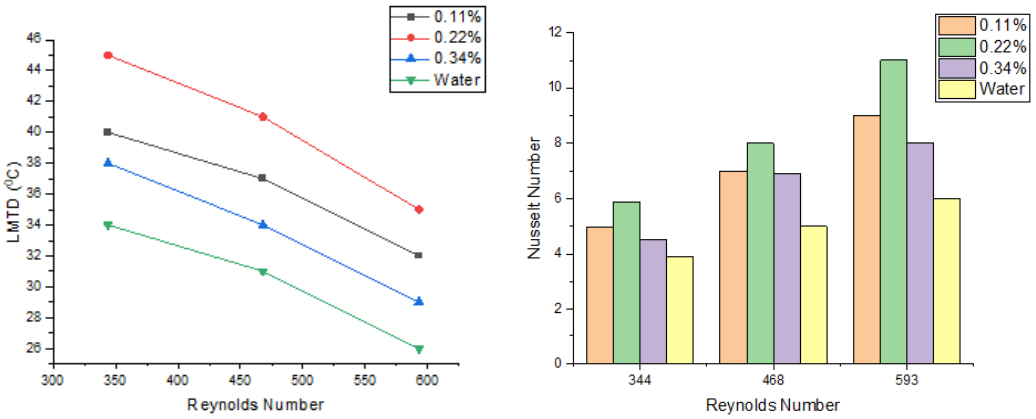

Figure 6. (**a**) Relationship between logarithmic temperature difference and Reynolds number; (**b**) relationship between Nusselt and Reynolds numbers.

Figure 6a revealed that as the Re number decreased with higher nanoparticle concentrations, the LMTD tended to increase. This is evident from the LMTD values as shown in Figure 6a; the observed decrease in the Re number with increasing nanoparticle concentration in nanofluids was influenced by changes in fluid viscosity, altered flow characteristics, and the transition towards laminar flow regimes. An inverse relationship between the LMTD and the Reynolds number was observed and the results are aligned with the study [13]. Similarly, from Figure 6b it is observed that the Nu numbers tended to increase as the Re numbers increased, which represents the enhanced h due to the thinning of the thermal boundary layer and the increased flow rate of the fluid which incremented the Re number and increased the k. The hydrodynamic boundary layer developed on low

flow rates or low Reynolds numbers, and the region was equal to 2/3 of the tube length. Similarly, the thermal boundary layer thicknesses at concentrations of 0.11% were 0.32 mm, 0.275 mm, and 0.24 mm, respectively, at flow rates of 6, 8, and 10 LPM. This indicates that increased turbulence and mixing caused the thicknesses of the boundary layer to drop with the flow rate. The comparable thicknesses for a concentration of 0.22% were 0.37 mm, 0.323 mm, and 0.2875 mm, which continued the pattern of decreasing thickness as flow rates increased. The thicknesses were 0.438 mm, 0.375 mm, and 0.334 mm at the maximum concentration of 0.34%. These values decreased with the flow rate, but they were still greater than at lower concentrations because of the increased viscosity that hindered heat transmission and fluid movement. Distilled water consistently had lower boundary layer thicknesses than nanofluids, measuring 0.274 mm, 0.268 mm, and 0.209 mm at the same flow rates. This indicates that nanofluids have greater heat transmission capacities even if their viscosity is higher. Increasing the flow velocity generally results in a thinner thermal boundary layer and improves heat transfer. However, increased concentrations of nanoparticles thickened the boundary layer by increasing viscosity and boosting K simultaneously. As the concentrations increased, it led to a decrease in the Prandtl number due to a decrease in the heat capacity and an increase in the k, as the Prandtl number is dependent on the k. As the Prandtl number increased, it lead to the thinning of the boundary layer, and when the Prandtl number decreased, the boundary layer became thick. These trends are in line with these studies [15,16]. It was discovered that 0.22% was the best concentration for maximizing heat transfer, balancing increased thermal characteristics with controllable viscosity.

4. Conclusions

This study was conducted to evaluate the thermal behavior of a shell and tube H.X using water and nanoparticles at different concentrations, and it was noted that every property of the nanofluids provided better thermal conductivity (k) than distilled water. The k was improved by 26%, 44%, and 58% with nanoparticle concentrations of 0.11%, 0.22%, and 0.34%. The viscosity increased with the nanoparticle concentration but offset the thermal benefits at the highest concentration of 0.34%. It was noted that the U reached its maximum enhancement when the nanoparticle concentration was at its highest at 0.22%, where the U increased by over 33.33%, and at a 0.22% concentration, the h was 48% higher than the distilled water concentration. These findings show that nanoparticle loading enhances H.X convective heat transfer by 0.22%. Similarly, the $\dot{Q}$ also had the same characteristics enhanced with the highest value at a 0.22% concentration. By using up to this concentration of nanofluids, the $\dot{Q}$ was raised to about 30% when compared to the use of water, implying the effectiveness of dilated heat transmission with the help of nanofluids. The results showed that the U and h were most improved at 8 and 10 L/min flow rates, respectively, when the flow rate was increased. It was observed that the LMTD values were higher with higher concentrations of nanoparticles because as the Re number decreased, it resulted in laminar flow due to the viscosity of the fluid demonstrating being enhanced. The thermal boundary layer thicknesses at a concentration of 0.11% were 0.32 mm, 0.275 mm, and 0.24 mm, respectively, at flow rates of 6, 8, and 10 LPM. This indicates that increased turbulence and mixing caused the thicknesses of the boundary layer to drop with the flow rate. The comparable thicknesses for a concentration of 0.22% were 0.37 mm, 0.323 mm, and 0.2875 mm, which continued the pattern of decreasing thickness as flow rates increased.

Author Contributions: Conceptualization, S.I. and M.F.N.; methodology, S.I., Z.N. and T.K.; validation, A.T., M.A.B. and M.M.; formal analysis, S.I., M.A.B. and M.M.; investigation, M.F.N., T.K. and Z.N.; data curation, S.I., M.F.N. and M.M.; writing—original draft preparation, M.F.N., M.A.B. and S.I.; writing—review and editing, A.T., S.I. and M.M.; supervision, S.I. and M.M.; project administration, S.I. and A.T. All authors have read and agreed to the published version of the manuscript.

Funding: This research received no external funding.

Institutional Review Board Statement: Not applicable.

Informed Consent Statement: Not applicable.

Data Availability Statement: Data are contained within the article.

Acknowledgments: All the authors are thankful to the MED department for their support.

Conflicts of Interest: The authors declare no conflicts of interest.

References

1. Barzegarian, R.; Aloueyan, A.; Yousefi, T. Thermal performance augmentation using water based Al_2O_3-γ nanofluid in a horizontal STHX under forced circulation. *Int. Commun. Heat Mass Transf.* **2017**, *86*, 52–59. [CrossRef]
2. Godson, L.; Deepak, K.; Enoch, C.; Raja, B.R.J.; Raja, B. Heat transfer characteristics of silver/water nanofluids in a STHX. *Arch. Civ. Mech. Eng.* **2014**, *14*, 489–496. [CrossRef]
3. Shahrul, M.; Mahbubul, I.M.; Saidur, R.; Sabri, M.F.M. Experimental investigation on Al_2O_3-W, SiO_2-W and ZnO-W nanofluids and their application in a STHX. *Int. J. Heat Mass Transf.* **2016**, *97*, 547–558. [CrossRef]
4. Li, Q.; Xuan, Y. Convective heat transfer and flow characteristics of Cu-water nanofluid. *Sci. China Ser. E Technol. Sci.* **2002**, *45*, 408–416. [CrossRef]
5. Liu, M.S.; Lin, M.C.C.; Huang, I.T.; Wang, C.C. Enhancement of thermal conductivity with CuO for nanofluids. *Chem. Eng. Technol.* **2006**, *29*, 72–77. [CrossRef]
6. Subramanian, R.; Kumar, A.S.; Vinayagar, K.; Muthusamy, C. Experimental analyses on heat transfer performance of TiO_2–water nanofluid in double-pipe counter-flow heat exchanger for various flow regimes. *J. Therm. Anal. Calorim.* **2020**, *140*, 603–612. [CrossRef]
7. Farajollahi, B.; Etemad, S.G.; Hojjat, M. Heat transfer of nanofluids in a STHX. *Int. J. Heat Mass Transf.* **2010**, *53*, 12–17. [CrossRef]
8. Albadr, J. Thermal Performance of STHX Using PG/Water and Al_2O_3 Nanofluid. In *Advances in Heat Exchangers*; IntechOpen: London, UK, 2019. [CrossRef]
9. Anitha, S.; Thomas, T.; Parthiban, V.; Pichumani, M. What dominates heat transfer performance of hybrid nanofluid in single pass STHX. *Adv. Powder Technol.* **2019**, *30*, 3107–3117. [CrossRef]
10. Shaker, M.; Birgersson, E.; Mujumdar, A.S. Extended Maxwell model for the thermal conductivity of nanofluids that accounts for nonlocal heat transfer. *Int. J. Therm. Sci.* **2014**, *84*, 260–266. [CrossRef]
11. Einstein, A. Investigations on the Theory of the Brownian Movement. 1956. Available online: https://books.google.com.au/books/about/Investigations_on_the_Theory_of_the_Brow.html?id=AOIVupH_hboC&redir_esc=y (accessed on 18 March 2024).
12. Pak, B.C.; Cho, Y.I. Hydrodynamic and Heat Transfer Study of Dispersed Fluids with Submicron Metallic Oxide Particles. *Exp. Heat Transf. Int. J.* **1998**, *11*, 151–170. [CrossRef]
13. Sohel, M.R.; Khaleduzzaman, S.S.; Saidur, R.; Hepbasli, A.; Sabri, M.F.M.; Mahbubul, I.M. An experimental investigation of heat transfer enhancement of a minichannel heat sink using Al_2O_3-H_2O nanofluid. *Int. J. Heat Mass Transf.* **2014**, *74*, 164–172. [CrossRef]
14. Sparrow, E.M.; Gregg, J.L. Laminar-free-convection heat transfer from the outer surface of a vertical circular cylinder. *Trans. Am. Soc. Mech. Eng.* **1956**, *78*, 1823–1828. [CrossRef]
15. MacDevette, M.M.; Myers, T.G.; Wetton, B. Boundary layer analysis and heat transfer of a nanofluid. *Microfluid. Nanofluidics* **2014**, *17*, 401–412. [CrossRef]
16. Poply, V.; Singh, P.; Chaudhary, K.K. Analysis of laminar boundary layer flow along a stretching cylinder in the presence of thermal radiation. *Wseas Trans. Fluid Mech.* **2017**, *8*, 159–164.

Disclaimer/Publisher's Note: The statements, opinions and data contained in all publications are solely those of the individual author(s) and contributor(s) and not of MDPI and/or the editor(s). MDPI and/or the editor(s) disclaim responsibility for any injury to people or property resulting from any ideas, methods, instructions or products referred to in the content.